

New Organic Semiconductors for Stable, High-Performance Organic Thin-Film Transistors

Kazuo Takimiya¹, Eigo Miyazaki¹, Tatsuya Yamamoto, Takafumi Izawa¹

¹Dept. of Applied Chemistry, Graduate School of Engineering, Hiroshima University, Higashi-Hiroshima, 739-8527, Japan

TEL:+81-82-424-7734, e-mail: ktakimi@hiroshima-u.ac.jp

Keywords : OTFTs, New Organic Semiconductors, Heteroarenes, Stability, High-Performance

Abstract

Novel sulfur-containing aromatic compounds were developed as stable, high-performance organic semiconductors for OTFT applications. Of them, dinaphtho[2,3-b:2',3'-f]thieno[3,2-b]thiophene (DNNT) consisting of six aromatic rings gave high quality thin films by vapor deposition, which acted as a superior FET channel showing FET mobility as high as $3.0 \text{ cm}^2 \text{ V}^{-1} \text{ s}^{-1}$. On the other hand, highly soluble 2,7-dialkyl[1]benzothieno[3,2-b][1]benzothiophenes (C_n -BTBTs) gave solution-processible OTFTs with FET mobility higher than $1.0 \text{ cm}^2 \text{ V}^{-1} \text{ s}^{-1}$.

1. Introduction

Recent prevailing interests in organic electronics have encouraged synthetic chemists to develop new organic semiconductors as an active material for various electronic device applications such as organic light emitting diodes (OLEDs), organic thin-film transistors (OTFTs), and photovoltaic cells.¹ One of such organic semiconductors recently developed is 2,7-diphenyl[1]benzothieno[3,2-b]benzothiophene (DPh-BTBT, Fig. 1) that gives high-performance OTFTs with field-effect mobility (μ_{FET}) higher than $1.0 \text{ cm}^2 \text{ V}^{-1} \text{ s}^{-1}$ under ambient conditions.² In addition, their superior device characteristics were preserved for long period of time (~250 days) without significant degradation. For these reasons, DPh-BTBT is one of the best p-channel OTFT active materials so far reported. Thus, it is interesting to develop new materials based on the structure of DPh-BTBT by modifications of its chemical structure. In accordance with this concept, we have designed two novel target organic semiconductors based on the benzothieno[3,2-b]benzothiophene (BTBT) core structure, namely, 2,7-dialkyl[1]benzothieno[3,2-b][1]benzothiophenes (C_n -BTBTs)³ as highly soluble semiconductors suitable to the solution-processed OTFTs and dinaphtho[2,3-b:2',3'-f]thieno[3,2-b]thiophene (DNNT)⁴ as a highly

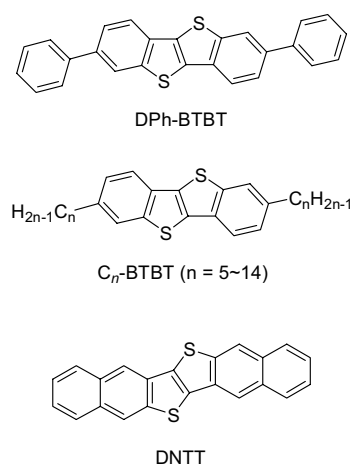


Fig. 1 Chemical structures of new OTFT materials.

π -extended rigid heterophene for vapor-processed OTFTs (Fig. 1).

2. Results and discussion

C_n -BTBTs as soluble molecular semiconductors for solution processed OTFTs: π -conjugated polymers with aromatic and/or heteroaromatic backbones, represented by poly(3-hexylthiophene) (P3HT), have been conventionally utilized as soluble organic semiconductors for solution-processed OTFTs.⁵ Recently, the very high μ_{FET} of $0.7 \text{ cm}^2 \text{ V}^{-1} \text{ s}^{-1}$ and the current on/off ratio ($I_{\text{on}}/I_{\text{off}}$) of 10^6 were reported for solution-processed OTFTs possessing the thieno[3,2-b]thiophene-thiophene copolymer based active semiconducting channel.⁶ For further improvement of device performance, however, polymer materials may not be suitable because they inherently have uncertainty in the structure such as statistical distribution of molecular weight and structural defects

caused by mislinkage of monomers, which may act as carrier traps in the semiconducting channel.

In this regard, molecular materials are advantageous in terms of their well-defined structure, ease of purification, and controllable properties. In fact, impressive examples of molecular-based solution-processed OTFTs showing μ_{FET} as high as $1.0 \text{ cm}^2 \text{ V}^{-1} \text{ s}^{-1}$ were recently reported using soluble pentacene (TIPS-pentacene) and anthradithiophene derivatives, in which bulky 2-(trialkylsilyl)ethynyl substituents at the peri position (*the molecular short-axis direction*) act as solubilizing groups.⁷

Our target molecular semiconductors, C_n -BTBTs, on the other hand, have two solubilizing long alkyl groups at *the molecular long-axis direction* of the BTBT core. This molecular design strategy, in contrast to that of TIPS-pentacene, will facilitate lateral intermolecular interaction of the BTBT core to enhance large molecular overlap, realizing the enhancement of performance in OTFTs.

A series of C_n -BTBTs were easily synthesized.^{3,8} Thus obtained C_n -BTBTs are quite soluble in common organic solvents; the experimentally determined solubilities in chloroform at rt are listed in TABLE 1. Derivatives with C_5H_{11} – C_9H_{19} groups are almost freely soluble, while those with alkyl groups longer than $C_{12}H_{25}$ showed reduced solubilities.

Homogeneous thin films were deposited on a Si/SiO₂ substrate by spin-coating using a 0.4 wt% solution of C_n -BTBT in chloroform. The spin-coated thin films were highly crystalline as indicated by X-ray diffraction (XRD) measurements: as a representative, an XRD pattern of C_{12} -BTBT thin film is shown in Fig. 2, where a series of peaks assignable to (00 l) reflections were clearly observed, and the

TABLE 1. Characteristics of C_n -BTBTs and their devices fabricated on Si/SiO₂ substrates.

n	Solubility ^a / $g L^{-1}$	d -spacing / \AA	μ_{FET}^b / $\text{cm}^2 \text{ V}^{-1} \text{ s}^{-1}$	$I_{\text{on}}/I_{\text{off}}$
5	60	22.8	0.16–0.43	10^8
6	70	24.5	0.36–0.45	10^8
7	70	27.1	0.52–0.84	10^7
8	80	29.0	0.46–1.80	5×10^7
9	90	31.6	0.23–0.61	10^8
10	24	33.3	0.28–0.86	10^8
11	13	35.9	0.73–1.76	10^7
12	8.6	37.5	0.44–1.71	10^8
13	5.0	40.2	1.20–2.75	10^7
14	2.3	41.8	0.19–0.72	10^8

^a concentration of saturated solution in chloroform at rt.

^b data from more than 10 devices.

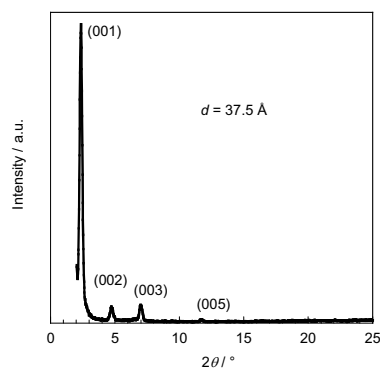
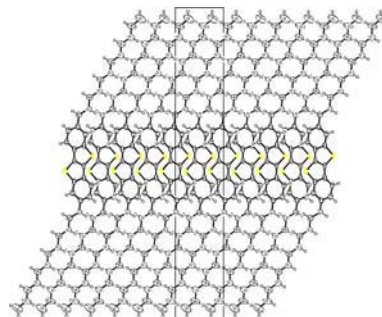


Fig. 2. XRD pattern of C_{12} -BTBT.

inter-layer distance (d -spacings) calculated from these reflections is 37.5 \AA . d -Spacings of the other derivatives depended on the length of the alkyl groups: with longer alkyl groups, larger d -spacings were obtained (TABLE 1), indicating that all the derivatives take similar molecular packing structures.

Gold source and drain electrodes (80 nm) were vapor-deposited on top of the thin films through a shadow mask to complete fabrication of OTFT devices with channel length (L) and width (W) of $50 \mu\text{m}$ and 1.5 mm , respectively. TABLE 1 summarizes the FET characteristics of the devices evaluated under ambient conditions without any precautions to

(a)



(b)

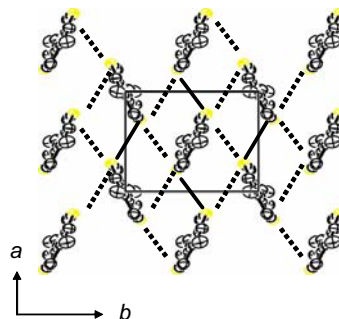


Fig. 3. Crystal structure of C_{12} -BTBT: (a) b -axis projection (b) molecular packing pattern in the BTBT layer. Intermolecular S–S contacts were designated as solid lines (3.54 \AA) or dotted line (3.63 \AA).

eliminate air and moisture. Regardless of the length of the alkyl groups, thin films of C_n -BTBT derivatives acted as a superior semiconducting channel, and μ_{FET} of the devices was higher than $0.1 \text{ cm}^2 \text{ V}^{-1} \text{ s}^{-1}$. Although no pronounced dependence of μ_{FET} on the alkyl length was observed, C_n -BTBT with alkyl groups longer than the $C_{10}H_{21}$ group tended to show higher mobility than derivatives with shorter alkyl groups. Note that the mobility of $2.8 \text{ cm}^2 \text{ V}^{-1} \text{ s}^{-1}$ is one of the best reported so far among solution-processed OFETs.

In order to understand the high performance of C_n -BTBT-based TFT devices, we carried out single-crystal X-ray structural analysis of C_{12} -BTBT. As shown in Fig. 3a, the crystal assumes a ‘layer-by-layer’ structure consisting of alternately stacked aliphatic layers and BTBT core layers. In the BTBT core layer, the molecules take herringbone-type packing (Fig. 3b) to facilitate 2D carrier transport property. In addition, a network of intermolecular interactions through short S–S contacts (3.54 and 3.63 Å) exists in the BTBT core layer. Since the existence of 2D semiconducting layers with strong intermolecular overlap is considered to be one of the prerequisites to realizing high-performance OTFTs,⁹ the high mobility of C_n -BTBT-based TFT devices is well understood.

DNTT, rigid and highly π -extended heterophene with six fused-aromatic rings for vapor-processed OTFTs: as well-documented by the OTFTs based on oligoacenes (pentacene and naphthacene), rigid and highly π -extended molecular semiconductor, i.e. pentacene,¹⁰ affords OTFTs with better performances than those of less π -extended naphthacene.¹¹ In this regard, extension of the BTBT core with annulated benzene rings affording the structure of DNTT is very intriguing, compared to the simple attachment of phenyl substituents, i.e. the structure of DPh-BTBT. We thus focused on DNTT as a promising candidate for high performance OTFT active material. However, the synthetic methods for such highly π -extended heteroarens have not been established. Although there could be several possible synthetic approaches to the target including tedious multi-step syntheses, we developed a new straightforward synthetic route that starts from a commercially available naphthalene derivative and construct the central heteroaromatic rings at the final step (Fig. 4).

DNTT was isolated as thermally stable yellow crystals that are readily purified by recrystallization or vacuum sublimation. Fig. 5 shows the solution UV-vis spectra of DNTT. Its optical HOMO-LUMO gap

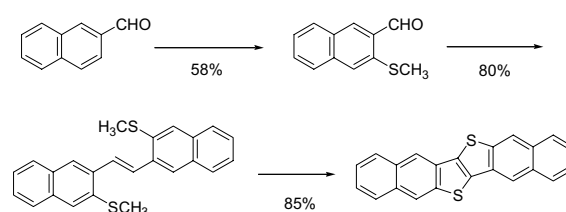


Fig. 4. Three-step synthesis of DNTT.

estimated from the absorption edges is determined to be ca. 3.0 eV. In addition, chemical stability of DNTT was tested: DNTT solution was saturated with air, and the UV-vis spectra were periodically measured. Even after 48 h no detectable change in UV-vis spectra was observed (Fig. 5). We thus conclude that DNTT is a highly stable organic semiconductor, similar to DPh-BTBT and C_n -BTBTs.

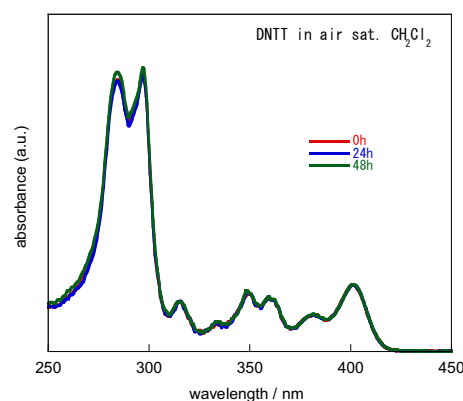


Figure 5. UV-vis absorption spectra of DNTT.

OTFT studies were carried out using ‘‘Top-contact’’-type devices with $W/L = \text{ca. } 30$, which were fabricated by vacuum deposition on Si/SiO₂ substrates whose surfaces were treated with hexamethyldisilazane (HMDS), octyltrichlorosilane (OTS), or octadecyltrichlorosilane (ODTS). All the

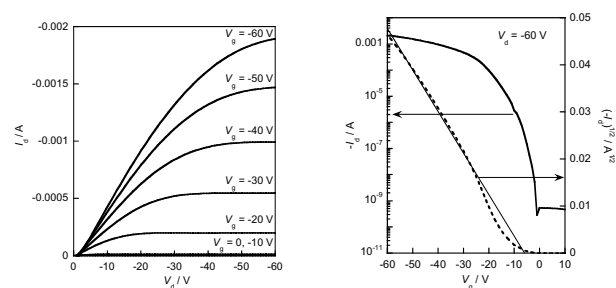


Fig. 6. FET characteristics of DNTT-based OFET on ODTS-treated substrate ($T_{\text{sub}} = 60 \text{ }^\circ\text{C}$): output characteristics (left) and transfer characteristics at $V_d = -60 \text{ V}$ (right).

TABLE 2. FET characteristics of DNTT devices fabricated on Si/SiO₂ substrates with different surface treatments and under different substrate temperatures (T_{sub}).

Surface-treatment reagent	T_{sub} °C	μ_{FET}^a cm ² V ⁻¹ s ⁻¹	$I_{\text{on}}/I_{\text{off}}$
HMDS	rt	0.73–0.83	5×10^6
	60	1.1–1.2	5×10^6
	100	1.1–1.3	10^7
OTS	rt	1.6–1.8	10^7
	60	2.1–2.9	10^7
	100	1.6–1.9	10^7
ODTS	rt	1.1–1.3	10^6
	60	2.1–3.0	5×10^6
	100	2.4–3.1	5×10^6

^a data from more than 10 devices.

devices fabricated under various conditions showed typical p-channel FET characteristics with μ_{FET} higher than $0.7 \text{ cm}^2 \text{ V}^{-1} \text{ s}^{-1}$ and $I_{\text{on}}/I_{\text{off}} > 10^6$ evaluated under ambient conditions (Fig. 6 and TABLE 2). In particular, excellent FET characteristics with μ_{FET} higher than $2.0 \text{ cm}^2 \text{ V}^{-1} \text{ s}^{-1}$ and $I_{\text{on}}/I_{\text{off}}$ of 10^6 were observed for the devices fabricated on the OTS- or ODTS-treated substrates.

3. Summary

Considering the stability, performances of the devices, and easy accessibility (synthetic easiness), we believe that DNTT can be a potential candidate for a “post-pentacene” material, a vapor-processible organic semiconductor of the next generation. On the other hand, C_n-BTBTs are highly soluble organic semiconductors that give solution-processed OTFT devices with the highest mobility so far attained among solution-deposited OTFTs. This means that conventional conjugated polymers are not only the choice for developing superior solution-processed OTFTs; properly designed small π -extended molecules with solubilizing groups are also very intriguing.

4. References

- (a) H. Klauk (ed.), *Organic Electronics, Manufacturing and Applications*, Wiley-VCH: Weinheim (2006). (b) see also a special issue on organic electronics: S. A. Jenkhe, *Chem. Mater.* **2004**, 16, 4381.
- K. Takimiya, H. Ebata, K. Sakamoto, T. Izawa, T. Otsubo, and Y. Kunugi, *J. Am. Chem. Soc.* **128**,

- 12604 (2006).
- H. Ebata, T. Izawa, E. Miyazaki, K. Takimiya, M. Ikeda, H. Kuwabara, and T. Yui, *J. Am. Chem. Soc.* **129**, 15732 (2007).
- T. Yamamoto and K. Takimiya, *J. Am. Chem. Soc.* **129**, 2224 (2007).
- (a) Z. Bao, A. Dodabalapur, and A. J. Lovinger, *Appl. Phys. Lett.* **69**, 4108 (1996). (b) B. S. Ong, Y. Wu, P. Liu, and S. Gardner, *J. Am. Chem. Soc.* **126**, 3378 (2004). (c) M. Heeney, C. Bailey, K. Genevicius, M. Shkunov, D. Sparrowe, S. Tierney, and I. McCulloch, *J. Am. Chem. Soc.* **127**, 1078 (2005). (d) H. Pan, Y. Li, P. Liu, B. S. Ong, and S. Zhu, G. Xu, *J. Am. Chem. Soc.* **129**, 4112 (2007).
- I. McCulloch, M. Heeney, C. Bailey, K. Genevicius, I. Macdonald, M. Shkunov, D. Sparrowe, S. Tierney, R. Wagner, W. Zhang, M. L. Chabiny, R. J. Kline, M. D. McGehee, and M. F. Toney, *Nature Mater.* **5**, 328 (2006).
- (a) M. M. Payne, S. R. Parkin, J. E. Anthony, C.-C. Kuo, and T. N. Jackson, *J. Am. Chem. Soc.* **127**, 4986 (2005). (b) K. C. Dickey, J. E. Anthony, and Y.-L. Loo, *Adv. Mater.* **18**, 1721 (2006). (c) S. K. Park, T. N. Jackson, J. E. Anthony, and D. A. Mourey, *Appl. Phys. Lett.* **91**, 063514 (2007).
- B. Kořata, V. Kozmik, J. Svoboda, V. Novotná, P. Vanák, and M. Glogarvá, *Liq. Cryst.*, **30**, 603 (2003).
- J. Cornil, D. Beljonne, J.-P. Calbert, and J.-L. Brédas, *Adv. Mater.* **13**, 1053 (2001).
- (a) Y. Y. Lin, D. J. Gundlach, S.F. Nelson, and T. N. Jackson, *IEEE Electron Device Lett.* **18** (1997) 606. (b) T. W. Kelly, L. D. Boardman, T. D. Dunbar, D.V. Muires, M. J. Pellerite, and T. P. Smith, *J. Phys. Chem. B* **107** (2003), 5877.
- D. J. Gundlach, J. A. Nichols, L. Zhou, and T. N. Jackson, *Appl. Phys. Lett.*, **80**, 2925 (2002).